

tivities of protection against earthquakes, are seismic observations.

S. I. Subbotina Institute of Geophysics of NAS provides activity of a seismic stations network, which actually performs the role of the national seismological network for providing information for all seismic protection works. The network provides standardized data on seismic manifestations on the territory of Ukraine. On these data the evidence-based forecasts of seismic hazard values are determined. It is necessary for central and local authorities to ensure the stable development of the seismic regions, as well as for the research institutes of other ministries and agencies working in related industries of earthquake-resistant design and construction.

Results of seismic observations are widely used in solving problems in key directions of fundamental research of IGPh of NAS: the study of the tectonics, structure, geodynamics, and evolution of continental and oceanic lithosphere; construction three-dimensional integrated geophysical and petrophysical models of geological structures in order to predict mineral development and introduction of new

technological systems for processing and interpreting geophysical data; geophysical studies of the environment in order to predict seismic hazards and other threats to natural phenomena. Geodynamic processes that are constantly changing stress-strain state of geological environment, not only in seismically active zones, but as it is now scientifically proven, in the territories of ancient platforms of planet, requires permanent monitoring tools.

The integration of seismic and other geophysical studies can learn communication geophysical fields with the preparation of strong earthquakes sources.

Conclusion. Earthquake-resistant design and development of anti-seismic measures require knowledge of the quantitative parameters of the real seismic hazard and seismic data on the vulnerability of structures. The main link supplying objective data for activities to protect against earthquakes are seismological observation.

To obtain reliable baseline data is necessary to ensure the further expansion (increase in the number and uniformity of the distribution) network of seismic stations and its reequipment by modern equipment and software.

References

- [http://upload.wikimedia.org/wikipedia/ru/2/22/Tectonic_plates\(rus\).png](http://upload.wikimedia.org/wikipedia/ru/2/22/Tectonic_plates(rus).png)
- http://neic.usgs.gov/neis/eq_depot/2010/eq_100112_rja6/neic_rja6_w.html
- <http://earthquake.usgs.gov/eqcenter/shakemap/global/shake/2010rja6/>
- http://www.rbc.ua/rus/newsline/show/mezhamerikanskiy_bank_razvitiya_ushcherb_prichinennyi_emletryaseniem_gaiti_mozhet_dostigat_14_mlrd_doll_16022010
- Seismic zoning of the USSR. (Methodological framework and regional description of the 1978 map) // Eds. V. I. Bune, G. P. Gorshkov. — Moscow: Nauka, 1980. — 308 p. (in Russian).*
- State building codes SBC B.1.1-12: 2006 "Building in seismic regions of Ukraine". — Kiev: Ministry of Construction, Architecture and Housing and Communal Services of Ukraine, 2006. — 84 p. (in Russian).*

Melt segregation and matrix compaction: closed governing equation set, numerical models, applications

© Ya. Khazan¹, O. Aryasova¹, 2010

Institute of Geophysics, National Academy of Sciences of Ukraine, Kiev, Ukraine
ykhazan@gmail.com; oaryasova@gmail.com

Partially molten systems are commonly modeled as an interpenetrating flow of two viscous liquids and are therefore described in terms of fluid mechanics [Drew, 1983; McKenzie, 1984; Nigmatulin, 1990]. In the gravitational field a liquid filling a viscous permeable porous matrix is in mechanical equilibrium only if its pressure gradient is equal to the hydrostatic one, and the pressures of the liquid

and matrix are the same. If the liquid and matrix densities differ, with the liquid forming an interconnected network, the two conditions cannot be satisfied simultaneously, and the liquid segregates from the matrix while the latter compacts. The averaged momentum and mass conservation equations for a multi-phase medium are formulated separately for every phase. Considering the energy conservation

equation, this results in $4N+1$ equations for a N -phase medium while the number of unknowns is $5N$ ($3N$ velocity components, N pressures, temperature, and $N-1$ independent phase fractions). Therefore, for the problem to be fully determined it becomes necessary to add $N-1$ coupling equations. Khazan (2010; on review at GJI) and Khazan and Aryasova (Rus. Earth Phys., 2010, in press) derived a general equation (the mush continuity equation, MCE) closing the governing equation set. Its simplified 1D form valid for a two-phase system in the case of low-melt-fraction mush and linear matrix rheology, together with equation describing the rate of the inelastic porosity change [Scott, Stevenson, 1986], constitute a closed subset of governing equation set:

$$\frac{\partial}{\partial z} \frac{k(\varphi)}{\mu} \left(\frac{\partial(p_l - p_m)}{\partial z} - \Delta\rho g \right) = \varphi \frac{p_l - p_m}{\eta},$$

$$\frac{\partial\varphi}{\partial t} = \varphi \frac{p_l - p_m}{\eta}, \quad (1)$$

where p_l and p_m are the melt and matrix pressure, respectively, φ is the melt fraction or porosity, $k(\varphi) \propto \varphi^n$ is the matrix permeability, $\Delta\rho = \rho_m - \rho_l$ is the difference between the matrix, ρ_m , and melt, ρ_l , densities, η and μ are matrix and melt viscosities, correspondingly, $n=2$ to 3 , g is acceleration due to gravity; Z axis points upward. Let L be the thickness of the partially molten zone, and φ_0 be the maximum of the initial porosity distribution. In terms of dimen-

sionless coordinate $\zeta = z/L$, time $\tau = t\Delta\rho g L/\eta$, melt overpressure $\Pi = (p_l - p_m)/\Delta\rho g L$, and porosity $\psi = \varphi/\varphi_0$, the equations may be written as

$$\frac{\partial}{\partial \zeta} \psi^n \left(\frac{\partial \Pi}{\partial \zeta} - 1 \right) - \gamma_c \psi \Pi = 0, \quad \frac{\partial \psi}{\partial \tau} = \psi \Pi,$$

where

$$\gamma_c = \frac{L^2}{\delta_c^2}, \quad \delta_c = \sqrt{\frac{k(\varphi_0)\eta}{\varphi_0\mu}}, \quad (2)$$

γ_c and δ_c are referred to as the compaction/segregation parameter and length, respectively. If coordinate is normalized by the compaction length, the first of Eqs. (2) does not contain γ_c [Grègoire et al., 2006] but it appears instead in the boundary conditions.

In what follows two characteristic situations referred to as segregation and compaction are considered. The former is a model of the evolution of a bounded partially molten zone. Its outer boundary coincides with solidus where the porosity and pressure difference vanish. The boundary and initial conditions are $\Pi(\tau, 0) = \Pi(\tau, 1) = 0$, $\varphi(0, \zeta) = 4\zeta(1 - \zeta)$. For compaction (of bottom sediments, e. g.), it is assumed that the bottom is impermeable, and porosity at $\tau=0$ is the same throughout the layer, so that: $\partial\Pi(\tau, 0)/\partial\zeta = 1$, $\Pi(\tau, 1) = 0$, $\psi(0, \zeta) = 1$.

The solutions to Eqs. (2) are shown in Fig. 1 for segregation, and Fig. 2 for compaction. One may

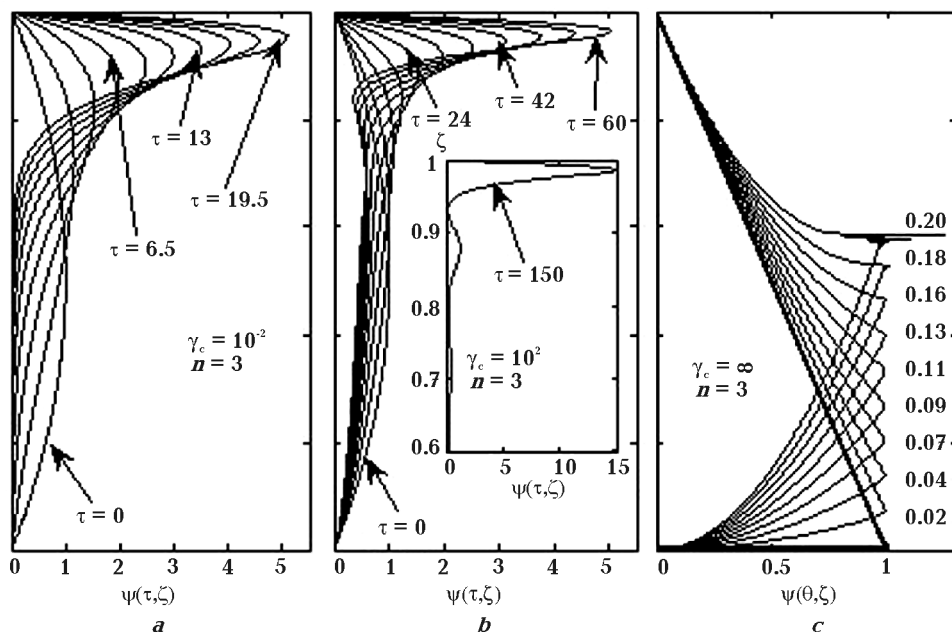


Fig. 1. Evolution of porosity $\psi(\tau, \zeta)$ at segregation: *a* — $\gamma_c = 10^{-2}$, *b* — $\gamma_c = 10^2$, *c* — at $\gamma_c \rightarrow \infty$ Eqs. (2) reduce to $\Pi=0$, $\partial\psi/\partial\zeta|_{\theta=0} = -\partial\psi^n/\partial\zeta$ with θ being a formally introduced time variable $\theta = \gamma_c \tau$. Note that the first and the second waves at $\tau = 150$ (*b*, inset) contain 57 and 13 % of the melt, respectively, with the rest of the melt residing in the tail.

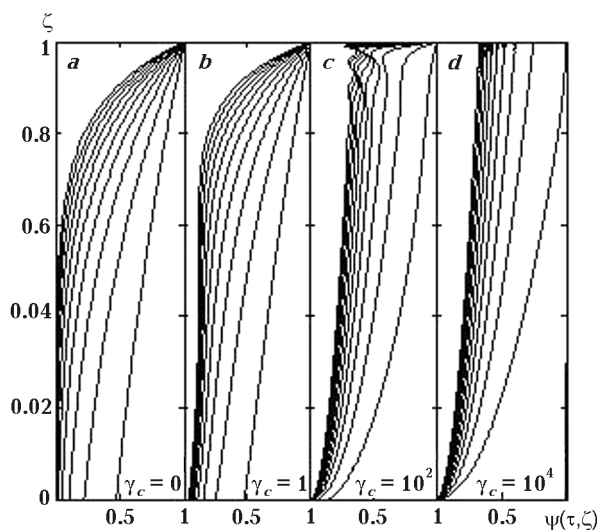


Fig. 2. Compaction of the bottom sediments at: *a* — $\gamma_c = 0$, *b* — $\gamma_c = 1$, *c* — $\gamma_c = 10^2$, *d* — $\gamma_c = 10^4$ ($n = 3$).

see from Fig. 1 that at low \tilde{a}_c practically all the melt segregates to the roof with amplitude of the porosity growing with time (Fig. 1, *a*). The pressure gradient remains hydrostatical in the enriched layer and evolves to zero in the low-melt fraction tail. At high γ_c (Fig. 1, *b*) a wave structure develops with the dimensionless pressure being generally low and sign reversible, and a significant part of the melt remaining trapped in the tail. The case $\gamma_c = \infty$ (Fig. 1, *c*) corresponds to $\Pi \equiv 0$ (or $p_l = p_m$). The porosity amplitude remains the same (i. e. no segregation occurs), and it takes $\partial\psi/\partial\zeta$ a finite time to reach the -8 implying a numerical instability, which is absent from the finite γ_c models. The variation of porosity while a liquid is expelled from a compacting porous layer (Fig. 2) is similar to that at segregation indicating that a property to generate a wave-like structure becomes more pronounced with increasing γ_c , i. e. at high melt viscosity. A large pluton layering [Wager, Brown, 1968] may be due to this wave structure, which is supported by the observation [Brown, 1973] that layered intrusions are commonly intrusions of a tholeiitic basalt while those of the alkali basalt parentage are rare, which may be due simply to about an order higher viscosity of the tholeiitic magmas.

The dependence of characteristic compaction, τ_c and segregation, τ_s , times on γ_c , is shown in Fig. 3. In dimensional variables an approximate fit to these results may be written as follows:

$$t_c \approx 2.49 \frac{\eta}{\Delta\rho g L} + \frac{L}{V_D}, \quad t_s \approx 19.5 \frac{\eta}{\Delta\rho g L} + 0.25 \frac{L}{V_D},$$

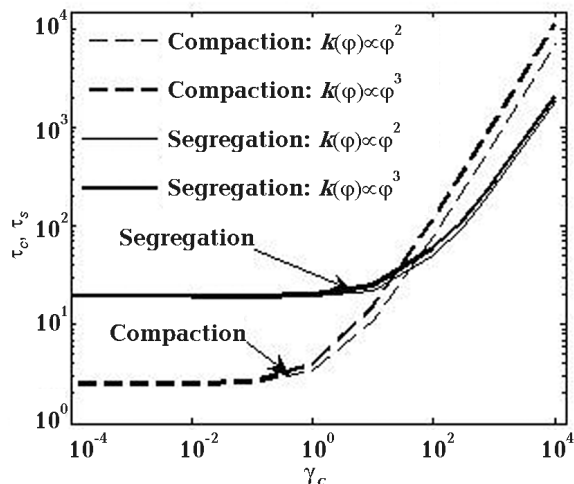


Fig. 3. Characteristic time of compaction τ_c and segregation τ_s , vs. γ_c .

$$V_D = \frac{\Delta\rho g k(\varphi_0)}{\mu\varphi_0}, \quad (3)$$

where V_D is the Darcy's velocity. The L^{-1} scaling of the compaction/segregation times at low γ_c effectively constrains the thickness of compacting porous sediments as well as the maximum possible thickness of the partially molten zone. Really, if the mushy layer thickness increases gradually, due to, for instance, sedimentation with a rate of r_d then the steady sediment thickness, L_d , may be estimated as $L_d/r_d = t_c$ wherefrom $L_d \approx 1.7\sqrt{\eta r_d / \Delta\rho g}$. Similarly, let a protokimberlite melt result from a decompression melting of a diapir floating at a velocity V_d with its temperature varying along an adiabat. The melting starts when the diapir top reaches the intersection level of the adiabat and solidus, and maximum possible thickness of the molten zone, L_s , may be estimated as $L_s \approx 4.5\sqrt{\eta V_d / \Delta\rho g}$. The estimates of L_d and L_s are valid if $\gamma_c \gg 2$ for the compaction problem or $\gamma_c \gg 80$ for a segregation one. Also, Darcy's velocity is to be large, namely $V_D \gg r_d$ at compaction and $V_D \gg 0.25V_d$ at segregation. These estimates relate to an evolution of a porous layer filled with a low viscosity liquid, and may be used to estimate, for instance, a steady thickness of porous marine sediments, or a maximum possible thickness of a partially molten zone filled with a low viscosity magma (kimberlite, carbonatite) at the moment of segregation. To illustrate the latter case, adopt the following parameter values: $\eta = 10^{19}$ Pas, $\Delta\rho = 100$ kg·m $^{-3}$, $V_d = 3$ cm·y $^{-1}$, $k(\varphi) = a^2\varphi^3/270$ [Wark et al., 2003], grain size $a = 1$ mm, $\varphi_0 = 0.01$, $\mu = 0.1$ Pas. Then compaction/

segregation length $\delta_c = 6$ km, $V_d = 30$ cm·y⁻¹, $t_s = 0.2$ My, $L_s = 8$ km, $\gamma_c = 1.7$. As soon as melt segregates, new partially molten zone grows, and the sequence of the events repeats until the whole diapir passes by the melting level. A diapir size, D , can be estimated based upon diameters $D = 20$ to 80 km of low-amplitude uplifts known to correlate

with kimberlite fields [Kaminsky et al., 1995]. Therefore, the decreasing dependence of the segregation time on a mushy layer thickness implies formation of clusters of $D/L_s = 3$ to 10 low volume eruptions of almost the same age and composition. An attractive feature of the model is that it relates the kimberlite origin to a localized incipient melting.

References

- Brown P. E.* A layered plutonic complex of alkali basalt parentage; the Lilloise Intrusion, East Greenland // *J. Geol. Soc. London.* — 1973. — **129.** — P. 405—418.
- Drew D. A.* Averaged field equations for two-phase flow // *Ann. Rev. Fluid Mech.* — 1983. — **15.** — P. 261—291.
- Grégoire M., Rabinowicz M., Janse A. J. A.* Mantle mush compaction: A key to understand the mechanisms of concentration of kimberlite melts and initiation of swarms of kimberlite dykes // *J. Petrol.* — 2006. — **47.** — P. 631—646.
- Kaminsky F. V., Feldman A., Varlamov V., Boyko A., Olofinsky L., Shofman I., Vaganov V.* Prognostication of primary diamond deposits // *J. Geochem. Explor.* — 1995. — **53.** — P. 167—182.
- McKenzie D.* The generation and compaction of partially molten rock // *J. Petrol.* — 1984. — **2.** — P. 713—765.
- Nigmatulin R. I.* Dynamics of multi-phase media. — New York: Hemisphere, 1990. — **1.** — 507 p.
- Scott D. R., Stevenson D. J.* Magma ascent by porous flow // *J. Geophys. Res.* — 1986. — **91.** — P. 9283—9296.
- Wager L. R., Brown G. M.* Layered Igneous Rocks. — Edinburgh, London: Oliver, Boyd, 1968. — 588 p.
- Wark D., Williams C., Watson E., Price J.* Reassessment of pore shapes in microstructurally equilibrated rocks, with implications for permeability of upper mantle // *J. Geophys. Res.* — 2003. — **108(B1).** — DOI:10.1029/2001JB001575.

Interactive visualization of large-scale numerical simulations with GPU-CPU systems

© M. Knox, P. Woodward, 2010

Laboratory of Computational Science and Engineering,
University of Minnesota, Minneapolis,
MN, USA

We present a method for pipelining results from large-scale fluid dynamical simulations in such a way as to exploit the exponentially increasing computational capacity of the latest generation of multi-core CPUs, many-cores and GP-GPUs. Exploiting this technique, together with an integration with several data post-processing and visualization utilities has enabled numerical experiments in computational fluid dynamics to be performed interactively on a new, dedicated system in our lab at the University of Minnesota. This method provides an immediate, user controlled visualization of the resulting

flows on the LCSE PowerWall display as well as through a globally accessible html and java web interface. The code restructuring required to achieve the necessary computational performance boost, as well as the interactive visualization are described. Requirements for these techniques to be applied to other codes are discussed, and our plans for tools that will assist programmers elsewhere to exploit these techniques are briefly described. Examples showing the capability of the new system and software are given for various applications in turbulent hydrodynamics, stellar flows, and mantle convection.